Energy-minimized conformation of gramicidin-like channels. I. Infinitely long poly-(L,D)-alanine $\beta^{6.3}$-helix

Hiroshi Monoi
Department of Physiology, Tohoku University School of Medicine, Sendai, Japan 980

ABSTRACT The energy-minimized conformation of an infinitely long poly-(L,D)-alanine in single-stranded $\beta^{6.3}$-helix was calculated by the molecular mechanics method. When energy minimization was started from a wide range of initial geometries, six optimized conformations were obtained and identified as the right- and left-handed counterparts of the $\beta^{4.5}$-, $\beta^{6.3}$-, and $\beta^{8.2}$-helices. It was found that their conformation energies increase in this order, the $\beta^{4.5}$-helix having the lowest energy. The backbone dihedral angles of the energy-minimized $\beta^{6.3}$-helix were: $\phi_L = -116°$ (or $-131°$), $\psi_L = 122°$ (or $111°$), $\phi_D = 131°$ (or $116°$), $\psi_D = -111°$ (or $-122°$), $\omega_L = 173°$ (or $173°$), and $\omega_D = -173°$ (or $-173°$) for the right-handed (or left-handed) helix. This helix was composed of 6.30 residues/turn with a pitch of 4.97 Å. All the α-carbons of L- and D-configurations appeared on one common circular helix. Interestingly, small deviations ($\sim 7°$) of the peptide bonds from the planar structure caused a considerable lowering of the conformation energy, and, at the same time, they produced more favorable fitting of the hydrogen bonds; the carbonyl oxygens and the nearest-neighbor α-hydrogens also took more favorable relative positions.

INTRODUCTION

This manuscript reports the energy-minimized conformation of infinitely long poly-(L,D)-alanine in single-stranded $\beta^{6.3}$-helix. This structure has been calculated by the molecular mechanics method.

The β-helix has a sequence of alternating L- and D-amino acids, its repeating unit being a dipeptide. It can be classified into three categories: single-stranded, parallel double-stranded, and antiparallel double-stranded β-helices. Each of the three can possess a right- or left-handed helix sense. In a right-handed β-helix, the amino and carbonyl groups of L-amino acids point toward the N-terminal end of the helix, whereas those groups of D-amino acids look toward the C-terminal end, thus consecutive hydrogen-bonds alternately facing in opposite directions. In a left-handed β-helix, the orientation of those functional groups is reversed. (In what follows, the hydrogen bonds involving the amino groups of L-amino acids will tentatively be referred to as "type I," whereas those involving the amino groups of D-amino acids, as "type II.")

Gramicidin A is a linear polypeptide antibiotic consisting of 15 amino acids, with alternating L- and D-configurations. Its terminal ends are blocked by a formyl residue at the N-terminal and by an ethanolamine residue at the C-terminal. The ion-conducting channel formed by gramicidin A in lipid bilayers is known to be a head-to-head (i.e., N-terminal-to-N-terminal) dimer of two gramicidin monomers, each of which is in single-stranded $\beta^{6.3}$-helix structure (1–7). The helix sense of the peptide backbone of the gramicidin channel has still been an enigma, although recent evidences favor the right-handedness (8–14).

The peptide backbone of the gramicidin channel is expected to be deformed, compared with that of the ideal β-helix (i.e., an infinitely long β-helix having noninteractive sidechains), mainly due to the occurrence of channel ends and to the presence of different kinds of larger sidechains which will be more or less interactive, and also due to the presence of water molecules within the channel.

Alanine is the simplest of the amino acids that possess asymmetric α-carbons. An infinitely long poly-(L,D)-alanine β-helix will involve only a small, if any, sidechain effect, and, obviously, there is no end effect. This helix without explicit presence of other molecules will correspond to a least-perturbed β-helix structure. The aim of the present work is to calculate the energy-minimized conformation of this peptide in an infinitely long single-stranded $\beta^{6.3}$-helix. The resultant conformation can also be used as a starting geometry to get the minimized structure of the more involved gramicidin channel.

METHODS

Molecular mechanics force field. The force field employed for the present molecular mechanics calculations was basically that of ECEPP83 (15), which is an improved version of ECEPP (16). But modifications have been made concerning the hydrogen-bond force field.

In ECEPP83, the conformation energy is given by

$$E = E_{ES} + E_{NB} + E_{TOR}, \quad (1)$$

where E_{ES} is the electrostatic energy, E_{NB} is the energy of nonbonded interactions, and E_{TOR} is the torsional energy of bonds. The nonbonded interactions are expressed by Lennard–Jones-type terms.

In the original form of ECEPP83 force field, the hydrogen-bond energy is composed of an electrostatic term and a Lennard–Jones-type interaction. The hydrogen-bond force field involves no explicit angular dependence, and it also gives considerably small energies to the hydrogen bond between the amino and carbonyl groups. In the present work, the hydrogen-bond terms were modified on the basis of preliminary ab initio SCF results on interactions of small molecules.

In the modified hydrogen-bond force field used in this work, the Lennard–Jones-type term of the hydrogen bond is expressed as

Address correspondence to Dr. Hiroshi Monoi, Department of Physiology, Tohoku University School of Medicine, Seiryocho 2-1, Sendai, Japan 980.

0006-3495/93/01/036/08 $2.00

$$E_{HB} = \cos\theta'(A_{HB}/r^{12} - B_{HB}/r^6) + (1 - \cos\theta')(A/r^{12} - B/r^6), \quad (2a)$$

$$\theta' = \theta^{\alpha}(\pi/2)^{1-\alpha}, \quad (2b)$$

where r is the distance between the hydrogen and the acceptor, θ is the supplement of the donar–H–acceptor angle, and α is a constant which is specific for the type of hydrogen bonds and related to the degree of angular dependence. When $\theta \geq \pi/2$ radians, only the normal Lennard–Jones term is used (put $\theta' = \pi/2$ in Eq. 2a).

For the hydrogen bond between the amino and carbonyl groups of the peptide backbone, normal Lennard–Jones parameters A and B and hydrogen-bond parameters A_{HB} and B_{HB} assume the following values: A_{HB} = 1690 Å^{12} kcal/mol, B_{HB} = 90 Å^6 kcal/mol; A = 19100 Å^{12} kcal/mol, B = 124 Å^6 kcal/mol. For this type of hydrogen bond, α = 1.6 is appropriate. When α = 1, Eq. 2 reduces to an equation of the same type as used by Lavery et al. (17).

In the modified hydrogen-bond force field, the electrostatic term was also improved. For H and O atoms involved in a hydrogen bond between amino and carbonyl groups of the peptide backbone, the electrostatic energy was enhanced by 0.75 times that in the original ECEPP83 force field (this treatment is equivalent to decreasing the dielectric constant to 4/7 its original value [see below]). This enhancement was applied only for a H–O distance r_{HO} less than 2.1 Å. No enhancement was made for $r_{HO} > 3.5$ Å in order that the new force field may coincide with ECEPP83 force field at long distances. For the intermediate range, a smooth switching region was introduced. A sigmoidal switching function was tentatively used, but the use of functions of other forms did not affect the final minimum-energy conformation of β-helices.

In a β-helix, the amino and carbonyl groups of L-amino acid residues point toward one end of the helix, whereas those groups of D-amino acid residues look toward the other end. In the modified force field, the electrostatic interaction between a peptide amino group and the adjacent peptide carbonyl group that point toward the same end of the helix was enhanced by a factor of 0.3. (However, when values from 0 to 0.5 were used for this enhancement factor, we obtained practically the same minimum-energy structure.) No electrostatic enhancement was made for the 1,4-interactions.

Within the framework of the modified force field, the total interaction energy between hydrogen-bonded amino and carbonyl groups of the peptide backbone was 5.5 kcal/mol in the optimized $\beta^{6.3}$-helix, and the total interaction energy between two hydrogen-bonded amino acid residues (which are linked to each other through one hydrogen bond) was 4.8 kcal/mol in this helix.[1]

Dielectric constant. It was shown in a foregoing paper (18) that the peptide backbone of the β-structure has a dielectric constant ϵ of 10. Now suppose that a $\beta^{6.3}$-helix is placed in low dielectric circumstances whose ϵ is comparable to that of saturated hydrocarbons ($\sim$2), and that the inner cylindrical pore of the helix is filled with water. According to our preliminary electrostatic calculation on this system performed on the basis of a three-dielectric model (18), it can be assumed that the apparent ϵ for the interaction between two charges present in the backbone region is less than 4 (and, obviously, greater than 2).

This value is greater than the default value of ϵ (=2) in ECEPP83 force field. This default value, however, is employed in the present computation. This is because CNDO/2, which was used in the parameterization of ECEPP83, tends to give smaller values of atomic partial charges (16).

Residue-number-based nonbonded cutoff. In the present calculations, a special type of residue-based cutoff was used for calculating nonbonded and electrostatic interations. In this mode of nonbonded cutoff, it is supposed that only if one residue is apart from another residue (on the primary structure) by not-more-than-N_{cut} residues (including the two residues in question), every atom in the former residue will see the field due to every atom of the other residue. This will be referred to as "residue-number-based cutoff" or "cutoff at the N_{cut}-th residue."

A routine was added to the original ECEPP83 software to include this mode of cutoff. One of the values of N_{cut} appropriate for β-helices is 30. This, or greater values, were used throughout this study unless otherwise stated (also see the section entitled Effects of the mode of nonbonded cutoff).

Conformation energy of a dipeptide unit. Throughout this work, the conformation energy is represented by the energy of the dipeptide unit positioned in the middle of the helix that is composed of at least $2N_{cut}$ amino acid residues. The energy of a dipeptide unit can be defined as

$$\Sigma(E_{ES} \text{ and } E_{NB} \text{ between any pair of atoms within the unit}) + (1/2)\Sigma(E_{ES} \text{ and } E_{NB} \text{ between any atom of the unit and any outside it}) + \Sigma(E_{TOR} \text{ of any bond of the unit}). \quad (3)$$

In the limit of infinite peptide length, the conformation energy as defined here is equal to the total conformation energy of the polypeptide divided by the number of dipeptide units.

Obviously, one can eliminate the contribution of the end groups to the conformation energy defined above by adopting a peptide length not shorter than $2N_{cut}$ amino acid residues. Thus, any end groups can be used. To calculate the energy defined by Eq. 3, another routine was added to the original ECEPP83 software.

Energy minimization. A finite length of poly-(L,D)-alanine in single-stranded β-helix was energy-minimized. By employing the mode of nonbonded cutoff described above (the residue-number-based cutoff) and the notion of the conformation energy of a central dipeptide unit (see above), *the resultant optimized conformation and conformation energy (of a central dipeptide unit) corresponds to the optimized conformation and conformation energy (per dipeptide unit), respectively, of an infinitely long helix.*

In the ECEPP83 software, the energy minimization is performed by means of a QCPE (Quantum Chemistry Program Exchange) program VA04A (19), which utilizes an iterative descent technique for minimization.

Eight dihedral angles were adopted as the independent variables for energy minimization: ϕ_i, ψ_i, ω_i, and χ_i (i = L, D), where ϕ_i and ψ_i are the dihedral angles with respect to the N–C$^{\alpha}$ and the C$^{\alpha}$–C′ bond, respectively, of the backbone, and ω_i is the dihedral angle with respect to the peptide bond (cf. reference 20); subscripts L and D denote L- and D-isomers. The sidechain positions of L- and D-alanine are given by χ_L and χ_D, respectively. The bond lengths and angles were treated as constants (their magnitudes are those of ECEPP83 and ECEPP [16]). During energy minimization, each of the eight parameters was maintained the same for all the L- (or D-) amino acid residues. (This assumption does not hold for molecules such as gramicidin, which possesses a finite peptide length and a sequence of various amino acids.) For this purpose, a third routine was added to the ECEPP83 software.

Axis of a helix. The longitudinal axis of a helix was calculated by the least squares. The axis was defined as a line such that all the L-C$^{\alpha}$ atoms are at one distance from the line, and, at the same time, all the D-C$^{\alpha}$

[1] The difference between the original and the modified ECEPP83 force field was most pronounced when energy minimization was performed under the constraint of rigid planar peptide bonds. In the $\beta^{6.3}$-helix minimized by the original force field, the carbonyl and amino groups of L- (or D-) amino acids of the right- (or left-) handed counterpart were greatly inclined toward the axis of the helix (by $\sim$35°), whereas those groups of D- (or L-) amino acids were reoriented outward (by approximately the same degrees), so that no favorable hydrogen bondings were formed. (For the corresponding conformation by the modified force field, see the section entitled Energy minimization under the constraint of the rigid planar configuration of peptide bonds.)

TABLE 1 **Effects of the nonbonded-cutoff residue number N_{cut} on the energy-minimized conformation of an infinitely long poly-(L, D)-alanine β-helix**

N_{cut}	ϕ_L	ψ_L	ϕ_D	ψ_D	ω_L	ω_D	Energy*
			degrees				*kcal/mol*
Right-handed helix:							
8	−114.65	122.33	130.96	−111.10	173.45	−172.68	0.17
10	−114.86	122.36	131.08	−111.00	173.47	−172.75	0.09
14	−115.34	122.25	131.36	−110.66	173.48	−172.81	0.00
20	−115.47	122.24	131.44	−110.56	173.48	−172.84	0.00
30	−115.50	122.23	131.45	−110.55	173.48	−172.84	0.00
44	−115.51	122.23	131.46	−110.54	173.48	−172.84	0.00
60	−115.51	122.23	131.46	−110.54	173.48	−172.84	0.00
Left-handed helix:							
8	−130.96	111.10	114.65	−122.33	172.68	−173.45	0.17
10	−131.08	111.00	114.86	−122.36	172.75	−173.47	0.09
14	−131.36	110.66	115.34	−122.25	172.81	−173.48	0.00
20	−131.44	110.56	115.47	−122.24	172.84	−173.48	0.00
30	−131.45	110.55	115.50	−122.23	172.84	−173.48	0.00
44	−131.46	110.54	115.51	−122.23	172.84	−173.48	0.00
60	−131.46	110.54	115.51	−122.23	172.84	−173.48	0.00

The starting structure is $\phi_L = \psi_D = -120°$ (or $-140°$) and $\phi_D = \psi_L = 140°$ (or $120°$) for the right-handed (or left-handed) helix; the starting values of all other dihedral angles are taken to be 180°. The values for dihedral angles and energies are given especially to two decimal places to express the status of convergence. (The conformations given in this table correspond to $\beta^{6.3}$-helices.)

* Conformation energy per dipeptide unit, expressed relative to that of the right-handed helix at the greatest N_{cut} level. The initial conformation energy was 16.5 kcal/mol (per dipeptide unit).

atoms are at another distance from it. The two distances may be equal, or unequal, to each other. A routine for calculating this axis was also added to the original ECEPP83 software.

Computers. Numerical calculation was performed on an NEC ACOS-2200 computer and an NEC SX-2N supercomputer at the Computer Center of Tohoku University.

RESULTS AND DISCUSSION

Effects of the mode of nonbonded cutoff

In performing the energy minimization of large molecules, the interactions between nonbonded atoms are sometimes cut off abruptly at a finite distance (usually 10–20 Å). When this mode of nonbonded cutoff is employed, the resultant optimized conformation will depend more or less on the starting geometry (owing to the appearance of spurious local energy minima), and, in addition, the relative conformation energies of different structures of the same molecule often depend on the cutoff distance, so that the true lowest-energy state is usually difficult to find. We found that this is also the case for β-helices. The situation was not greatly improved, even when a smooth switching region of several ångströms was introduced around the cutoff point, although this mode of cutoff is frequently used.

In the present calculation, the residue-number-based cutoff, or cutoff at the N_{cut}-th residue, is used (see the Methods section). With this mode of cutoff, the energies of different conformations can be compared directly, so long as a large value of N_{cut} is used (see below), and a unique optimized conformation is reached from a wide range of starting geometries (see the next section).

Table 1 shows the effect of cutoff residue number N_{cut} upon the optimized conformation. In this table, the values of dihedral angles and energies are especially given to two decimal places to express the status of convergence. As seen from this table, the optimized dihedral angles and conformation energy converge rapidly with the increase in N_{cut}. They remain virtually unchanged for N_{cut} values greater than 20. In what follows, we use an N_{cut} value of 30 or greater.

It is also noted that at each cutoff level, the optimized conformations have the same conformation energies irrespective of the helix sense. The optimized dihydral angles agree with the following theoretical expectations:

$$\phi_L = -\phi'_D, \quad \psi_L = -\psi'_D, \tag{4a}$$

$$\phi_D = -\phi'_L, \quad \psi_D = -\psi'_L, \tag{4b}$$

$$\omega_L = -\omega'_D, \quad \omega_D = -\omega'_L, \tag{4c}$$

$$\chi_L = -\chi'_D, \quad \chi_D = -\chi'_L, \tag{4d}$$

where symbols, with and without a prime, designate left- and right-handed counterparts, respectively. (As is theoretically expected, a pair of infinitely long right- and left-handed helices that satisfy Eq. 4 always have the same conformation energies.)

Starting geometries and energy-minimized conformations

Three energy-minimized conformations were obtained for each of the right- and left-handed β-helices when en-

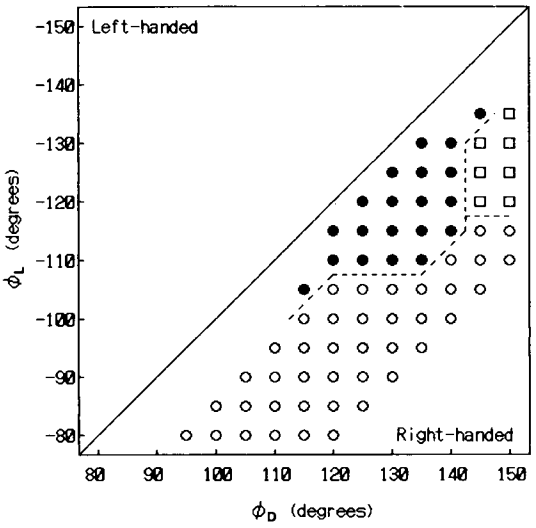

FIGURE 1 Starting geometries and energy-minimized conformations of infinitely long poly-(L,D)-alanine β-helices. The ordinate and abscissa represent starting values of ϕ_L and ϕ_D, respectively; starting values of other parameters are such that $\psi_L = \phi_D$, $\psi_D = \phi_L$, $\omega_L = \omega_D = \chi_L = \chi_D = 180°$. The same marks represent convergence to a common optimized conformation, which corresponds to a $\beta^{4.5}$-helix (○), $\beta^{6.3}$-helix (●), or $\beta^{8.2}$-helix (□); their dihedral angles are given in Table 2 (lines 1–6). Only right-handed helices are shown; the plots for left-handed helices are the mirror mirages of those for the right-handed helices with respect to the line $\phi_L = -\phi_D$.

ergy minimization was started from a wide range of initial geometries. They were identified as the $\beta^{4.5}$-, $\beta^{6.3}$-, and $\beta^{8.2}$-helices. This is shown below. (By starting from other initial structures, β-helices of higher orders were also obtained. But they will not be referred to here.)

Fig. 1 shows the effect of various starting values of ϕ_L and ϕ_D on energy minimization when starting values of other parameters were taken as $\psi_L = \phi_D$, $\psi_D = \phi_L$, and $\omega_L = \omega_D = 180°$. (Dihedral angles χ_L and χ_D for the sidechains were also put to be 180°, but the initial values of these angles did not affect the final conformation.) In this figure, various starting values of ϕ_L and ϕ_D are plotted, and different marks denote different optimized structures that were finally reached, the same marks representing convergence to a common optimized conformation. Only right-handed helices are plotted; the plots for left-handed ones are the mirror mirages of those for the right-handed helices with respect to the line $\phi_L = -\phi_D$. The range of the starting values examined was: $\phi_L = -80$ to -150, $\phi_D = 80$ to 150, and $\phi_L + \phi_D \leq 40°$ and $\geq -40°$, except for the case $\phi_L \sim -\phi_D$. (When $\phi_L \sim -\phi_D$, the conformation energy is extremely high, owing to the van der Waals overlap of adjacent atoms.)

As is immediately clear, the plots for each helix handedness can be divided into three groups, each of which corresponds to a unique optimized conformation. In Table 2 (lines 1–6), the dihedral angles of the three optimized conformations are given for both handednesses. These conformations are easily identified as the right-handed and left-handed counterparts of the $\beta^{4.5}$-, $\beta^{6.3}$-, and $\beta^{8.2}$-helices (also see the next section).

Table 3 lists values reported by several authors for the dihedral angles of the backbone of periodic $\beta^{6.3}$-helices. When energy minimization was started from these structures, only one optimized conformation was reached, and it is identical with the conformation that is labeled $\beta^{6.3}$-helix right-handed (or left-handed) in Table 2.

It is noteworthy that less stable local energy minima were not found in the course of energy minimization, in spite of the fact that a simple iterative descent algorithm was used for energy minimization. Only when minimization was started from outside the range of dihedral angles given above, local minima were often reached, but their energy levels were higher than those of the global minima by at least several kilocalories per mole of dipeptide unit.

Characteristics of the energy-minimized conformations of β-helices

Table 4 lists the values found for several parameters characterizing the three lowest-energy conformations of β-helices. (The values of the dihedral angles are given in

TABLE 2 **Dihedral angles of the energy-minimized conformations of infinitely long poly-(L,D)-alanine β-helices**

ϕ_L	ψ_L	ϕ_D	ψ_D	ω_L	ω_D	χ_L	χ_D	Identification
				degrees				
−86	106	123	−86	−171	174	−177	−178	$\beta^{4.5}$-helix right-handed
−116	122	131	−111	173	−173	−180	−179	$\beta^{6.3}$-helix right-handed
−125	134	134	−126	165	−165	−180	−180	$\beta^{8.2}$-helix right-handed
−123	86	86	−106	−174	171	178	177	$\beta^{4.5}$-helix left-handed
−131	111	116	−122	173	−173	179	180	$\beta^{6.3}$-helix left-handed
−134	126	125	−134	165	−165	180	180	$\beta^{8.2}$-helix left-handed
−127	132	135	−111	180	180	180	180	$\beta^{6.3}$-helix right-handed with rigid planar peptide bond*
−135	111	127	−132	180	180	180	180	$\beta^{6.3}$-helix left-handed with rigid planar peptide bond*

* Energy minimization was performed under the constraint of the rigid planar *trans* configuration of peptide bonding. Angles χ_L and χ_D were also fixed at 180°, but this assumption did not affect appreciably the optimized dihedral angles of the backbone.

TABLE 3 **Reported dihedral angles of the backbones of periodic $\beta^{6.3}$-helices**

Handedness	ϕ_L	ψ_L	ϕ_D	ψ_D	ω_L	ω_D	Method	Reference
				degrees				
right*	−100	120	140	−130	180‖	180‖	energy minimization	Venkatachalam & Urry (21)
left*	−140	130	100	−120	180‖	180‖	energy minimization	Venkatachalam & Urry (21)
left‡	−139	123	114	−125	—	—	energy minimization	Roux & Karplus (22)
left§	−133	116	120	−130	180‖	180‖	model building, not energy-minimized	Koeppe & Kimura (23)

* Among the sidechain atoms, only C^β atoms are considered; hence the peptide roughly corresponds to poly-(L,D)-alanine.
‡ Poly-(L,D)-alanine. Although ω_L and ω_D are also optimized, their final values are not given.
§ Peptide backbone with a tetrahedral N–C^α–C′ angle of 110.5°. The dihedral angles have been calculated from Cartesian coordinates.
‖ Fixed at 180°.

Table 2, lines 1–6.) In this table, the helix sense is not specified, since the same values are attributed to both the right-handed and corresponding left-handed helices.

As indicated in this table, the three optimized helices have 4.5, 6.3, and 8.2 residues per turn. The corresponding helical pitches decrease slightly in this order. The C′ and N atoms of each helix species appear at approximately the same distance from the axis of the helix. The C^α atoms appear at 0.5 Å outside from these atoms. The radii of the cylindrical pores within the helices are 0.7, 1.9, and 3.0 Å for the $\beta^{4.5}$-, $\beta^{6.3}$-, and $\beta^{8.2}$-species, respectively, when the van der Waals "closest-approach" radii of C′ and N atoms are assumed to be 1.5 Å. The conformation energies of the helices increase in this order; the $\beta^{4.5}$-helix is most stable (if the difference in entropy is not taken into consideration).

Dihedral angles ω_i showed small but definite deviations from 180° (Table 2, lines 1–6). That is to say, the peptide bonds in optimized β-helices are no longer in the planar configuration. Dihedral angles χ_i for alanine sidechains were only slightly different from 180°; i.e., the sidechain positions remain in close vicinity of the intrinsic potential minimum.

The optimized $\beta^{6.3}$-helix has 6.30 residues per turn, which is essentially the same as that reported previously (2, 22, 23). The pitch of the helix is 4.97 Å, slightly longer than those reported formerly (4.88 Å/turn [22], 4.85 Å/turn [23]).

Take the longitudinal axis of the helix to be the z-axis of the cylindrical-coordinate system. The $z(+)$-side is taken to be directed to the C-terminal of the peptide. In Fig. 2 *a* and *b*, the positions of the backbone atoms of the optimized $\beta^{6.3}$-helix are represented in terms of this coordinate system. In this figure, ρ (radial distance) and ϕ (directional angle around the z-axis) are plotted against the z coordinate.

Interestingly, all the C^α atoms, which alternately have the L- or D-configuration, are at the same distance (3.87 Å) from the axis, and are aligned with equal spacings (0.79 Å) along the z-axis (see Fig. 2 *a*). The relative rotation around the z-axis is practically the same (57.2°) for any pair of successive C^α atoms. That is to say, the two species of C^α atoms are positioned on a common circular helix. This can be seen in Fig. 2 *b*, where all the C^α atoms are aligned on one straight line.

With the right-handed helix, hydrogen bonds of type I (involving the amino groups of L-amino acids) are nearly parallel with the axis of the helix. The directions of the amino and carbonyl groups of hydrogen bonds of this type are deviated from the direction of the z-axis only by ~4° (see the first line in Table 5). Contrastingly, hydrogen bonds of type II (involving the amino groups

TABLE 4 **Helix parameters and conformation energies of energy-minimized conformations of infinitely long poly-(L,D)-alanine β-helices**

Helix	Number of residues per turn	Axial translation per turn	Distance from the axis*			radius of pore‡	Conformation energy§
			C^α	C′	N		
	/turn	*Å/turn*		*Å*		*Å*	*kcal/mol*
$\beta^{4.5}$	4.46	5.32	2.74	2.23	2.20	0.7	−0.6
$\beta^{6.3}$	6.30	4.97	3.87	3.36	3.35	1.9	0.0
$\beta^{8.2}$	8.23	4.87	4.99	4.47	4.50	3.0	3.3

All the values are for both of the right- and left-handed helices.
* Average of the distances for L- and D-amino acids.
‡ Represented as the radius of the inner cylindrical envelope for the van der Waals surfaces of C′ and N atoms of the backbone (the van der Waals "closest-approach" radii of C′ and N atoms are taken to be 1.5 Å).
§ Conformation energy per dipeptide unit, expressed relative to that of the $\beta^{6.3}$-helix.

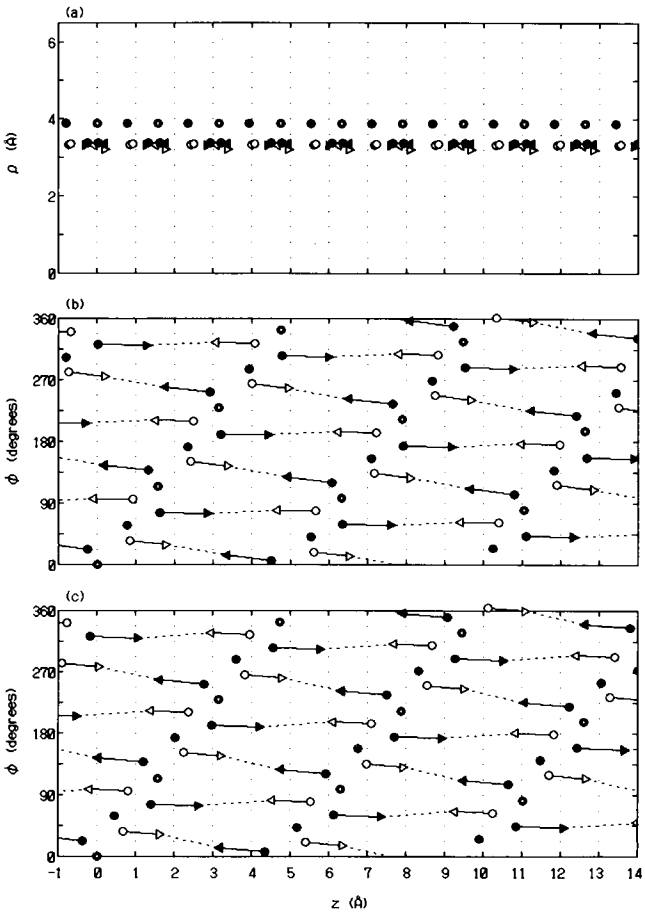

FIGURE 2 Cylindrical-coordinate plot of the energy-minimized poly-(L,D)-alanine $\beta^{6.3}$-helix (*a* and *b*). The bottom plot (*c*) represents the corresponding helix under the constraint of the rigid planar *trans* configuration of peptide bonds. Only the right-handed counterparts are shown. Ordinates ρ and ϕ are the radial distance and the azimuthal angle, respectively, in the cylindrical coordinate system; the longitudinal axis of the helix is taken as the *z*-axis. The origin is put at an L-C^{α} atom. The N-terminal end is to the left. The broken lines denote hydrogen bonds. ◎ and ◉ L- and D-C^{α}, respectively; O, amino N; ◁ and ▷, amino H of L- and D-amino acid; ●, carbonyl C; ◀ and ▶, carbonyl O of L- and D-amino acid.

of D-amino acids) are deviated from the direction of the axis by more than 20°. In the left-handed helix, the case is reversed with respect to the two types of hydrogen bonds, type II being nearly parallel with the axis.

Fig. 3 presents the space-filling model of the backbone of the optimized structure of the $\beta^{6.3}$-helix (right-handed). The lower figure in Fig. 3 is a longitudinal section of the helix, which has been cut off by a plane parallel with the surface of the page and containing the helix axis. Note the two types of hydrogen bonds with different orientations, one of which is nearly parallel with the axis of the helix.

The optimized conformation found above for the infinitely long $\beta^{6.3}$-helix is very regular, in marked contrast to the highly irregular structure of the gramicidin channel reported by Arseniev et al. (24). The latter structure has been constructed on the basis of NMR data and the molecular mechanics energy minimization. The difference between the two helices is attributable to the fact that the latter structure has a finite peptide length (hence a nonnegligible end effect is expected) and has a sequence of various amino acids. It may also be due to the presence of water molecules and ions within the latter channel. It may partly reflect the difference in molecular mechanics force field used in energy minimization. Arseniev et al. (24) employed ECEPP/2 force field (essentially an equivalent of ECEPP83 force field), whereas the force field adopted in the present calculation is a modified ECEPP83 force field (see the Methods section). (We found that the optimized β-structure tends to be irregular when energy minimization is performed by means of the original ECEPP83 force field.) The difference between the two helices may also reflect the fact that the NMR data of Arseniev et al. have been derived from the channel in a water-surfactant environment, whereas the present calculation postulates no explicit presence of other molecules.

Energy minimization under the constraint of the rigid planar configuration of peptide bonds

The peptide bond is often assumed to have a rigid planar configuration. As shown above (Table 2, lines 1–6), however, the peptide bonds of the lowest-energy β-helices exhibit a small but definite deviation from the planar configuration. It is interesting to see what is the opti-

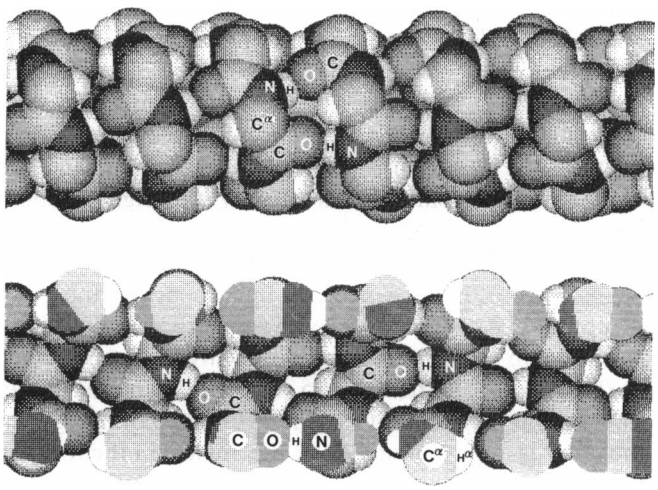

FIGURE 3 Space-filling representation of the backbone of the energy-minimized poly-(L,D)-alanine $\beta^{6.3}$-helix (right-handed). The N-terminal end is to the left. (Upper) Side view. (Lower) Longitudinal section, which has been cut off by a plane parallel with the surface of the page and containing the axis of the helix; it shows the inner surface of the frontal half of the upper figure. The radii of atoms used are: H, 1.00 Å; C, 1.50 Å; N, 1.45 Å; O, 1.35 Å.

TABLE 5 **Effects of the constraint of rigid planar peptide bonds on the energy-minimized conformation of infinitely long poly-(L,D)-alanine $\beta^{6.3}$-helix (right-handed)**

Constraint	Conformation energy*	Hydrogen bond					
		Type	H···O distance	θ‡	N–H direction§	C=O direction§	O–H$^{\alpha}$ distance‖
	kcal/mol		*Å*	*deg.*	*deg.*	*deg.*	*Å*
none	0.0	I	1.83	11	4.0 (L)	3.9 (D)	2.61 (D)
		II	1.82	11	22 (D)	21 (L)	2.63 (L)
$\omega_L = \omega_D = 180°$	1.1	I	2.01	25	8.7 (L)	9.1 (D)	2.40 (D)
		II	1.93	20	17 (D)	16 (L)	2.42 (L)

Optimized dihedral angles under the constraint are given in Table 2, lines 7–8. The letters L and D in parentheses denote that the atoms belong to L- and D-amino acids, respectively. With left-handed helices, hydrogen-bond types "I" and "II" should be replaced by "II" and "I," respectively, and "L" and "D" in parentheses, by "D" and "L."

* Conformation energy per dipeptide unit, expressed relative to that in the absence of the constraint.

‡ Supplement of the N–H–O angle.

§ Angle between the N–H (or C=O) bond and the helix axis.

‖ Distance between the carbonyl O atom of residue i and the α-H atom of residue ($i \pm 6$). The $\pm$ sign corresponds to whether or not the two atoms in question belong to D-amino acids.

mized structure when a rigid planar *trans* peptide linkage is always maintained. The results are summarized in Table 2 (lines 7–8), Table 5, and Fig. 2 *c*.

When energy minimization was performed under this constraint ($\omega_L = \omega_D = 180°$), the dihedral angles of the resultant $\beta^{6.3}$-helix (see Table 2, lines 7–8) were rather similar to the values reported by Koeppe and Kimura (23) for the $\beta^{6.3}$-structure, which has been made by a model building under the same constraint (Table 3). The energy-minimized helix was composed of 6.28 residues per turn with a pitch of 4.95 Å, in general agreement with the corresponding conformation in the absence of the constraint. However, the L-C$^{\alpha}$ and the D-C$^{\alpha}$ atoms were no more positioned on a common circular helix (Fig. 2 *c*). The L-C$^{\alpha}$ atoms appear at one distance (3.79 Å) from the axis, while the D-C$^{\alpha}$ atoms appear at a slightly different distance (3.90 Å) from the axis; and there is a shift in phase (+25° for D-C$^{\alpha}$ relative to L-C$^{\alpha}$) between the helical arrangements of the two atom species (values in parentheses are for the right-handed helix).

Remarkable differences between the optimized conformations in the presence and the absence of the constraint can be found concerning the hydrogen bonding. As shown in Table 5, the length of the hydrogen bonds of the latter conformation is 0.15 Å shorter than that of the former. The supplement θ of the hydrogen bond angle in the latter is approximately half the angle θ in the former (also compare Figs. 2 *b* and *c*). Clearly, the hydrogen bonds of the latter are energetically more favorable than those of the former. The lowering in the conformation energy amounts to 1.1 kcal/mol (per dipeptide unit). On the other hand, the concomitant change in ω_i is only $\pm 7°$ (Table 2). It is noticeable that small deviations of the peptide bonds from the planar configuration give rise to a considerable stabilization of the conformation.

The lowering of the conformation energy cannot fully be explained by the better fitting in hydrogen bonds alone. It must also be attributed to a subtle readjustment of the relative positions of atoms, by which the overall interactions between nonbonded atoms are made more favorable.

In this connection, we note the following observations. In the optimized $\beta^{6.3}$-helix under the constraint $\omega_L = \omega_D = 180°$, the interatomic distance between the carbonyl oxygen of residue i and the nearest-neighbor α-hydrogen (which belongs to residue $[i + 6]$ or residue $[i - 6]$) is 2.41 Å on average (Table 5), which corresponds to the distance of closest approach between the two atoms. The α-hydrogen, as a steric hindrance, unfavorably affects the hydrogen bond, leading to an ill-fitting in it. On the other hand, in the optimized $\beta^{6.3}$-helix without constraint, the corresponding distance is 2.62 Å on average (Table 5). The α-hydrogen at this distance is in the neighborhood of the minimum of the Lennard–Jones potential due to the carbonyl oxygen, and it is far from hindering the formation of an optimal hydrogen bond. This situation can be seen in Fig. 3 (note carbonyl oxygens and the nearest-neighbor α-hydrogens near the center of this figure).

With the ECEPP83 force field used in the present calculation, the bond lengths and the bond angles are constrained to be constant. According to the molecular dynamics study of Gunsteren and Karplus (25) on bovine pancreatic trypsin inhibitor, when both the bond lengths and angles are constrained, the dynamics of the molecule are considerably altered, and the magnitudes of the fluctuations of the atom positions and dihedral angles are reduced by a factor of two. The effect of the relaxation of bond lengths and angles on the energy-minimized conformation of β-helices remains to be examined.

The original ECEPP83 software is a gift from Dr. H. Chuman (Kureha Chemical Industry Co. Ltd., Tokyo, Japan) through JCPE (Japan Chemical Program Exchange), Tokyo, Japan (JCPE program No. P024).

Received for publication 9 March 1992 and in final form 17 September 1992.

REFERENCES

1. Wallace, B. A. 1986. Structure of gramicidin A. *Biophys. J.* 49:295–306.
2. Urry, D. W., M. C. Goodall, J. D. Glickson, and D. F. Mayers. 1971. The gramicidin A transmembrane channel: characteristics of head-to-head dimerized $\pi_{(L,D)}$ helices. *Proc. Natl. Acad. Sci. USA.* 68:1907–1911.
3. Urry, D. W., T. L. Trapane, and K. U. Prassad. 1983. Is the gramicidin A transmembrane channel single-stranded or double-stranded helix? A simple unequivocal determination. *Science (Wash. DC).* 221:1964–1967.
4. Weinstein, S., J. T. Durkin, W. R. Veatch, and E. R. Blout. 1985. Conformation of the gramicidin A channel in phospholipid vesicles: a fluorine-19 nuclear magnetic resonance study. *Biochemistry.* 24:4374–4382.
5. Arseniev, A. S., I. L. Barsukov, V. F. Bystrov, A. L. Lomize, and Yu. A. Ovchinnikov. 1985. ^{1}H-NMR study of gramicidin A transmembrane ion channel. Head-to-head right-handed, single-stranded helices. *FEBS (Fed. Eur. Biochem. Soc.) Lett.* 186:168–174.
6. Nicholson, L. K., and T. A. Cross. 1989. The gramicidin cation channel: an experimental determination of the right-handed helix sense and verification of β-type hydrogen bonding. *Biochemistry.* 28:9379–9385.
7. Hing, A. W., S. P. Adams, D. F. Silbert, and R. E. Norberg. 1990. Deuterium NMR of Val^1···(2-^{2}H)Ala^3···gramicidin A in oriented DMPC bilayers. *Biochemistry.* 29:4144–4156.
8. Urry, D. W., K. U. Prasad, and T. L. Trapane. 1982. Location of monovalent cation binding sites in the gramicidin channel. *Proc. Natl. Acad. Sci. USA.* 79:390–394.
9. Cornell, B. A., F. Separovic, A. J., Baldassi, and R. Smith. 1988. Phospholipid bilayers measured by solid state carbon-13 NMR. *Biophys. J.* 53:67–76.
10. Smith, R., D. E. Thomas, F. Separovic, A. R. Atkins, and B. A. Cornell. 1989. Determination of the structure of a membrane-incorporated ion channel. *Biophys. J.* 56:307–314.
11. LoGrasso, P. V., L. K. Nicholson, and T. A. Cross. 1989. N–H bond length determinations and implications for the gramicidin channel conformation and dynamics from ^{15}N–^{1}H dipolar interactions. *J. Am. Chem. Soc.* 111:1910–1912.
12. Chiu, S.-W., L. K. Nicholson, M. T. Brenneman, S. Subramaniam, Q. Teng, J. A. McCammon, T. A. Cross, and E. Jakobsson. 1991. Molecular dynamics computations and solid state nuclear magnetic resonance of the gramicidin cation channel. *Biophys. J.* 60:974–978.
13. Prosser, R. S., J. H. Davis, F. W. Dahlquist, and M. A. Lindorfer. 1991. ^{2}H nuclear magnetic resonance of the gramicidin A backbone in a phospholipid bilayer. *Biochemistry* 30:4687–4696.
14. Koeppe II, R. E., L. L. Providence, D. V. Greathouse, F. Heitz, Y. Trudelle, N. Purdie, and O. S. Andersen. 1992. On the helix sense of gramicidin A single channels. *Protein.* 12:49–62.
15. Chuman, H., F. A. Momany, and L. Schäfer. 1984. Backbone conformations, bend structures, helix structures and other tests of an improved conformational energy program for peptides: ECEPP83. *Int. J. Peptide Protein Res.* 24:233–248.
16. Momany, F. A., R. F. McGuire, A. W. Burgess, and H. A. Scheraga. 1975. Energy parameters in polypeptides. VII. Geometric parameters, partial atomic charges, nonbonded interactions, hydrogen bond interactions, and intrinsic torsional potentials for the naturally occurring amino acids. *J. Chem. Phys.* 79:2361–2381.
17. Lavery, R., H. Sklenar, K. Zakrzewska, and B. Pullman. 1986. The flexibility of the nucleic acids: (II) The calculation of internal energy and applications to mononucleotide repeat DNA. *J. Biomol. Struct. and Dynam.* 5:989–1014.
18. Monoi, H. 1991. Effective pore radius of the gramicidin channel. Electrostatic energies of ions calculated by a three-dielectric model. *Biophys. J.* 59:786–794.
19. Powell, M. J. D. 1965. VA04A: minimum of function of several variables. *QCPE* 11:60.
20. IUPAC-IUB Commission of Biochemical Nomenclature. 1970. Abbreviations and symbols for the description of the conformation of polypeptide chains. Tentative rules (1969). *Biochemistry.* 9:3471–3479.
21. Venkatachalam, C. M., and D. W. Urry. 1983. Theoretical conformational analysis of the gramicidin A transmembrane channel. I. Helix sense and energetics of head-to-head dimerization. *J. Comput. Chem.* 4:461–469.
22. Roux, B., and M. Karplus. 1991. Ion transport in a model gramicidin channel. Structure and thermodynamics. *Biophys. J.* 59:961–981.
23. Koeppe II, R. E., and M. Kimura. 1984. Computer building of β-helical polypeptide models. *Biopolymers* 23:23–38.
24. Arseniev, A. S., A. L. Lomize, I. L., Barsukov, and V. F. Bystrov. 1986. Gramicidin A transmembrane channel. Three-dimensional structure reconstruction based on NMR spectroscopy and energy refinement. *Biol. Membr.* 3:1077–1104. (In Russian).
25. van Gunsteren, W. F., and M. Karplus. 1981. Effect of constraints, solvent and crystal environment on protein dynamics. *Nature (Lond.).* 293:677–678.